Switchable Bidirectional/Unidirectional LWA Array based on Half-Mode Substrate Integrated Waveguide

Switchable Bidirectional/Unidirectional LWA Array based on Half-Mode Substrate Integrated Waveguide

Qingbi Liao, *Student Member, IEEE*, Lei Wang, *Senior Member, IEEE*,

***Abstract*—A novel leaky-wave antenna array with switchable radiation patterns is designed and manufactured at X-band based on a half-mode substrate integrated waveguide. It generates endfire and broadside radiation patterns in two orthogonal planes. The endfire radiation is bidirectional in the xz plane, and the broadside radiation is unidirectional in the yz plane. These two radiations can be controlled by triggering in-phase or out-of-phase port excitations. The excitations also enable the scanning beams to switch between xz and yz planes. A feeding network is designed with a 3-dB coupler and a phase tuner to generate the in-phase and out-of-phase excitations. In the feeding network, the phase difference is realized without using any phase shifter. The feeding network has two input ports, one for the in-phase excitation and one for the out-of-phase excitation. A prototype antenna was manufactured and tested to validate the concept.**

***Index Terms*—Beam scanning, leaky-wave antennas, substrate integrated waveguide (SIW), switchable radiation pattern.**

I. Introduction

Leaky-wave antennas (LWAs) rely their radiation properties on an adequate control of the propagation constant of the selected leaky mode [1]–[4]. Its radiation direction typically changes with the frequency, due to the frequency variations of the phase in the propagation mode. LWAs are categorized into two groups, depending on their guide-wave structures: periodic [5], [6], and uniform [3], [7]. Here, we focus on uniform guide-wave structures. Uniform LWAs, with a continuous perturbation, can be compressed by using a half-mode or half-width structure [8]–[10]. Their propagation properties are modified by changing the width of the half-mode waveguides.

Recently, LWAs have been implemented in substrate integrated waveguide (SIW) technology in order to reduce their manufacturing cost [7], [11], [12]. In SIW, these antennas are low profile, and can be easily integrated with planar circuits [13], [14]. Besides, SIW circuits can be reduced in size using a half-mode substrate integrated waveguides (HMSIW) as proposed in [15]. In [16]–[18], the propagation properties of HMSIWs were studied demonstrating that their losses are similar to full-mode SIWs. LWAs designed with HMSIW structures have been proposed to produce reconfigurable radiation patterns [19], quadri-polarization [17], [18], backfire-to-endfire beam scanning [20], propagation constant control [21], quasi-optical special multiplexer [22], and a parallel plate waveguide launcher [23]. The arrays of LWAs can be excited by an asymmetry feeding [24] or a higher order mode [18], [25], [26] to generate in-phase radiation patterns. The LWA arrays have been designed to realize wide-angle scanning [27], polarization diversity [28], and monopulse patterns for estimating direction of arrival (DoA) [29].

The phased-array LWAs capable of two dimensional scanning need complicated beam forming networks (BFN) and expensive phase shifters [30]. Single LWA element has the continuous frequency-scanning in the longitudinal plane. Together with phase shifters, the conventional phased-array LWAs such as in [31]–[33] can realize continuous phase-scanning in the transverse plane. The combination of continuous frequency-scanning and phase-scanning can realize the full-space or two dimensional scanning.

In this letter, we propose a solution to scan in two orthogonal longitudinal planes without using complicated BFN or phase shifters. A designed feeding network can provide 0 and π phase differences between the output ports. Since the feeding network has no continuous phase variation, the proposed antenna enables continuous frequency-scanning but not the continuous phase-scanning. The different phases enable the continuous frequency-scanning in two longitudinal planes, but no full-space or two dimensional scanning. The HMSIW LWA array with this feeding can alternate frequency-scanning between xz and yz planes. In the different longitudinal planes, the LWA array generates switchable radiation patterns, the bidirectional and unidirectional. This LWA array finds application in DoA estimation using the frequency-scanning property [29], new radio access platforms, such as satellites or high-altitude platforms, and airborne communication networks [34], in which a bidirectional pattern is required for inter-layer communications and a unidirectional one for downlink communications.

II. Antenna design and configuration

A. In-phase and Out-of-phase Feeding Network

The feeding network provides in-phase and out-of-phase excitations and is composed of four parts: input ports, a 3-dB coupler, a phase tuner, and output ports, as shown in Fig. 1a. The 3-dB coupler is based on an H-plane straight Y-junction [15] and provides a $\pi/2$ phase difference [17]. The phase tuner provides another $\pi/2$ phase difference by changing the width of half-mode waveguide [18]. The out-of-phase excitation is similar to the TE_{20} mode excitation in [26]. The output ports are added only for evaluation. The input ports, Port 1 and Port 2, determine the phase differences between the output ports, Port 3 and Port 4. Specifically, when Port 1 is excited, the phase difference between the output ports is 0, and when

Manuscript received May 22, 2020; revised xx; accepted xx.

Q. Liao is with the Division of Electromagnetic Engineering, KTH Royal Institute of Technology, SE 100 44 Stockholm, Sweden (e-mail: qlia@kth.se).

L. Wang is with the Institute of Sensors, Signals and Systems, Heriot-Watt University, Edinburgh, U.K. (e-mail: wanglei@ieee.org).

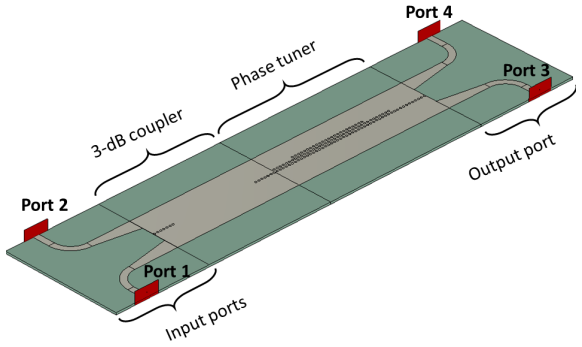

(a) Feeding network.

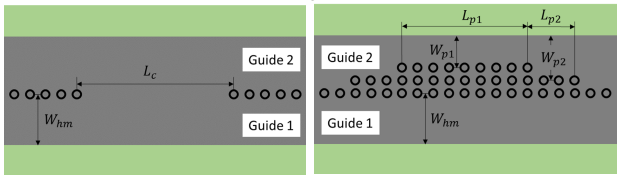

(b) 3-dB coupler. (c) Phase tuner.

Fig. 1: Half-mode in-phase and out-of-phase feeding network made of two input ports, a 3-dB coupler, a phase tuner, and two output ports.

Port 2 is excited, the phase difference is π. Therefore, we have two modes of operation, *in-phase* and *out-of-phase* modes. By switching between these two modes, the antenna array is fed with 0 or π phase differences and generates the bidirectional or unidirectional radiation patterns.

The 3-dB coupler is shown as in Fig. 1b. It has an HMSIW structure with a width W_{hm} equal to half the width of the complete SIW structure. The 3-dB coupler is based on an H-plane straight Y-junction [15]. As in Fig. 1b, the distance L_c between the central via walls is optimized to achieve a low return loss and reduce the coupling between input ports. The discontinuity of the central via walls bifurcates the electromagnetic waves evenly into the two waveguides, Guide 1 and Guide 2. We define $\Delta\phi_1$ as the phase shift from the coupler between Guide 1 and Guide 2. At the operating frequency, the phase shift $\Delta\phi_1$ is $-\pi/2$ at Port 1 excitation and $\pi/2$ at Port 2 excitation.

To have 0 or π phase differences, we design a phase tuner to generate another $\pi/2$ phase shift, depicted in Fig. 1c. In the phase tuner, we add two rows of the via walls in Guide 2 decreasing its width. The width of Guide 2 first tapers from W_{hm} to W_{p2}, and to W_{p1}, then it increases in an inverse way. The width of Guide 1 remains W_{hm}. In Guide 2, since the half TE_{10} mode propagates, the electromagnetic waves have different guided wavelengths λ_{p1}, λ_{p2}, and λ_{hm} corresponding to the waveguide widths W_{p1}, W_{p2} and W_{hm}. The guided wavelength in Guide 1 is also λ_{hm}. L_{p1} and L_{p2} are the lengths of Guide 2 with widths W_{p1} and W_{p2}. Then, the phase shift $\Delta\phi_2$ between Guide 1 and Guide 2 caused by the different widths is

$$\Delta\phi_2 = 2\pi L_{p1}\left(\frac{1}{\lambda_{hm}} - \frac{1}{\lambda_{p1}}\right) + 4\pi L_{p2}\left(\frac{1}{\lambda_{hm}} - \frac{1}{\lambda_{p2}}\right). \quad (1)$$

The lengths L_{p1} and L_{p2} are optimised to have a low return loss and a phase shift $\Delta\phi_2$ equal to $\pi/2$. The total phase difference is $\Delta\phi = \Delta\phi_1 + \Delta\phi_2$, the sum of the phase shifts of the power divider and phase tuner, and it is

$$\Delta\phi = \begin{cases} 0, & \text{Port 1 excitation,} \\ \pi, & \text{Port 2 excitation.} \end{cases} \quad (2)$$

With this configuration, the feeding network can provide 0 or π phase difference between the output ports by switching the excitation ports.

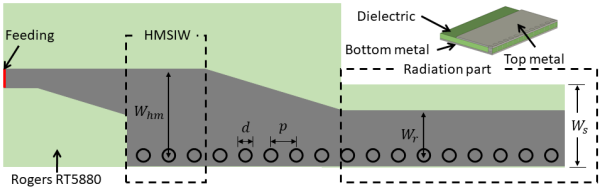

Fig. 2: The LWA antenna element. The inset is a piece of the radiation part.

B. Half-Mode LWA Array

The half-mode LWA array is composed of two antenna elements. One of the antenna elements is shown in Fig. 2. For the evaluation purpose, a microstrip feeding is connected to the element generating the half TE_{10} mode. The half-mode guiding structure is an open waveguide when its width is small [8]. The wave travelling along the waveguide with the width W_r starts to radiate through the open edge. To reduce the return loss, the width of the HMSIW tapers from W_{hm} to W_r. For the open waveguide, the leaky effect is mainly determined by the width. We optimize the width W_r so that the operating frequency is from 11 to 14 GHz. The parameters of the half-mode LWA antenna element are listed in TABLE I, where W_s is the width of the substrate, d is the diameter of vias, p is the spacing between vias, t is the thickness of the board, and ϵ_r is the relative permittivity of the substrate.

TABLE I: Parameters of the half-mode LWA element.

Parameters	W_{hm}	W_r	W_s	d	p	t	ϵ_r
Values (mm)	6.5	4.2	6.45	0.5	0.8	0.508	2.2

We place these two LWA elements back-to-back to construct the half-mode LWA array. This placement introduces a π phase difference when considering the combination of the radiation patterns. Apparently, the width of the waveguide W_r influences not only the leaky wave properties of the antenna elements, but also the LWA array factor AF expressed as [35],

$$AF = a_0 + a_1 e^{-j(k_0 \cdot r\cos\theta - \Delta\phi + \pi)}. \quad (3)$$

In Eq. (3), a_0 and a_1 are the electric amplitudes, k_0 is the wavenumber in free space, r is the distance between two elements, $\Delta\phi$ is the phase difference, 0 or π, provided by the feeding network, and the extra π is caused by the back-to-back construction. At the broadside direction, $\theta = \pi/2$, the array factor is simplified as $AF = a_0 + a_1 e^{-j(\Delta\phi+\pi)}$. That is, at the broadside direction, the radiation pattern has a minimum

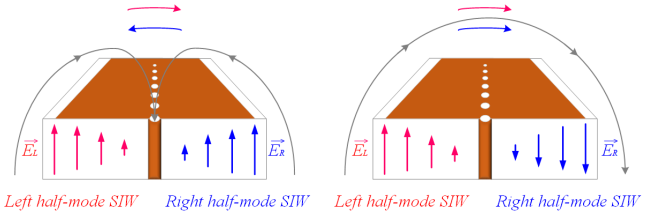

(a) Port 1 excitation. (b) Port 2 excitation.

Fig. 3: Illustration of the radiation principle based on the electric field distribution. (a) Electric field distribution in the bidirectional (endfire) LWA. (b) Electric field distribution in the unidirectional (broadside) LWA.

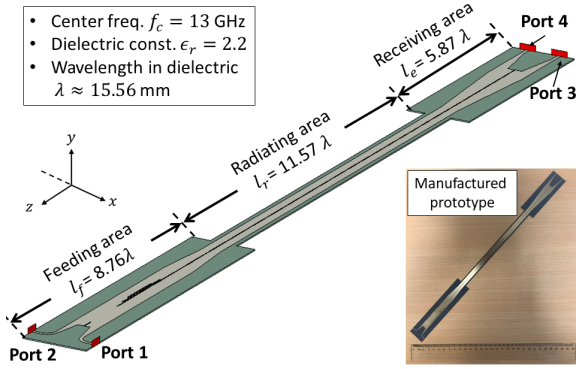

Fig. 4: The half-mode LWA array. Port 1 is the in-phase excitation and generates the bidirectional (endfire) radiation, and Port 2 is the out-of-phase excitation and generates the unidirectional (broadside) radiation. The subset shows the manufactured prototype.

when the phase difference $\Delta\phi$ is 0, and a maximum when $\Delta\phi$ is π [36].

To better illustrate the array's radiation patterns, we draw two diagrams in Fig. 3 showing the electric field distributions in the transverse plane. Fig. 3a represents the in-phase mode, where the electromagnetic waves inside the two half-mode waveguides have the same phase. Outside the waveguide, the electric field vectors at the center have opposite directions. The E-field vector from the left side (the red vector in Fig. 3a) counteracts the E-field vector from the right side (the blue vector in Fig. 3a), which leads to a minimum at the broadside direction and a maximum at the endfire direction. As a result, a bidirectional (endfire) radiation pattern is generated. Correspondingly, Fig. 3b shows the out-of-phase mode, where the maximum of the E-field is in the middle. The array generates a unidirectional (broadside) radiation pattern.

Finally, the half-mode LWA array is connected to the in-phase and out-of-phase feeding network. The output ports in the feeding network and the microstrip feeding of the antenna element are removed after evaluation. The structure of the complete antenna is shown in Fig. 4 with a photo of manufactured prototype in a subset. The chosen substrate is Rogers RT5880 with a permittivity ϵ_r 2.2 and thickness 0.508 mm.

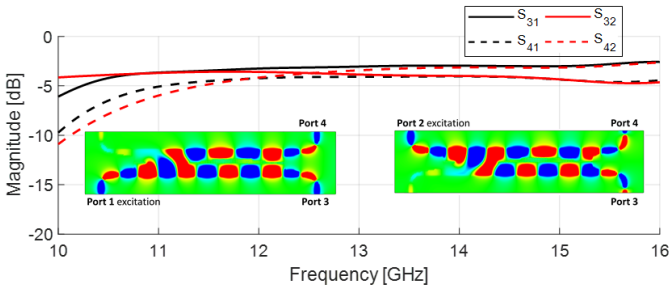

(a)

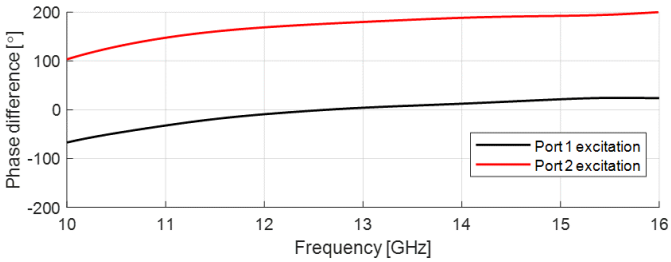

(b)

Fig. 5: (a) Simulated S parameters and electric fields of the feeding network in the in-phase (Port 1 excitation) and out-of-phase (Port 2 excitation) modes. (b) Phase differences between the output ports.

III. Simulation and Measurement Results

A. S Parameters of the Feeding Network

The magnitudes of the S parameters from simulations are plotted in Fig. 5a, where the black curves are the transmission coefficients of the Port 1 excitation, and the red curves correspond to the Port 2 excitation. In the frequency range from 12 to 14 GHz, the largest transmission coefficient is S_{31} with -3.11 dB $\pm$ 0.14 dB, and the smallest one is S_{41} with -4.14 dB $\pm$ 0.09 dB. This 1 dB difference comes from the phase tuner, where the narrow waveguides with the width W_{p1} and W_{p2} cause a leakage. Fig. 5b shows the phase differences between the output ports. In the in-phase mode, the phase difference is 4.11° at 13 GHz with $\pm$13.37° in the frequency range from 12 to 14 GHz, and in the out-of-phase mode, it is 179.94° with $\pm$11.08° in the same frequency range. The electric fields distributions at 13 GHz of the in-phase and out-of-phase modes can be observed in the two insets in Fig. 5a.

B. S Parameters of the Half-Mode LWA Array

The measured and simulated S parameters of the half-mode LWA array are depicted in Fig. 6. The measured reflection coefficients, $|S_{11}|$ and $|S_{22}|$, are larger than the simulated ones, but still below -10 dB in the frequency range from 11 to 14 GHz. The mutual coupling $|S_{21}|$ curves are below -15 dB and have a good agreement between the measurement and simulation. The mutual couplings and transmission coefficients of Port 1 and Port 2 excitations are similar, so that only the results of Port 1 are presented for clarity. The $|S_{41}|$ curve is similar to $|S_{31}|$, and it is omitted also. In the measurement

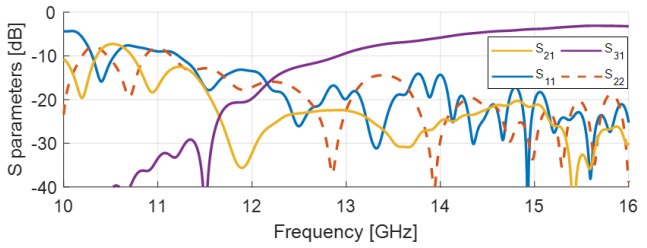

(a) Simulated results.

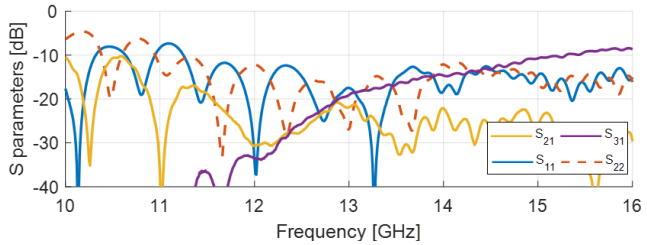

(b) Measured results.

Fig. 6: (a) Simulated and (b) measured S parameters of the half-mode LWA array.

results, the manufacturing inaccuracy and error might cause extra reflections and leakage.

C. Radiation Patterns

The feeding network provides 0 and π phase differences that generate the bidirectional (endfire) and unidirectional (broadside) radiation patterns. In Fig. 7, the measured radiation patterns at 12, 13, and 14 GHz are plotted in dash lines together with the simulation results in solid lines. The realized gains at these frequencies are listed in TABLE II. According to the antenna array theory, the realized gain of the broadside pattern (Port 2 excitation) is around 3 dB larger than the gain of the endfire pattern (Port 1 excitation). From TABLE II, we can observe that the gain of the Port 2 excitation is larger than the one of the Port 1 excitation. Their difference changes with the frequency.

TABLE II: Simulated realized gains of the LWA array.

Frequency [GHz]	12	13	14
Gain (Port 1) [dBi]	12.99	13.68	11.45
Gain (Port 2) [dBi]	14.69	15.48	15.95

There are two insets in Fig. 7 representing radiation patterns at 13 GHz. In Fig. 7a, the inset is the endfire radiation patterns from the Port 1 excitation. Two symmetrical beams are clearly observed in the radiation pattern. Due to the symmetry, only one beam is plotted out in Fig. 7a. The beam shapes of the measurement and simulation match well at these frequencies. The scanning plane of the dual beams is the xz plane and its scanning angle θ_1 grows from 33° to 57° as the frequency increases from 12 to 14 GHz. Correspondingly, in Fig. 7b, the inset is the broadside radiation patterns from the Port 2 excitation. The scanning plane is the yz plane and the scanning angle θ_2 increases from 30° to 59° as the frequency grows. Unfortunately, we observe a larger SLL in measured radiation

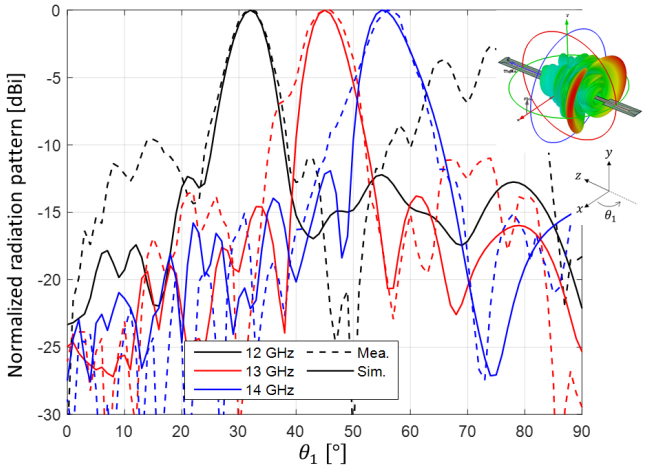

(a) Port 1 excitation.

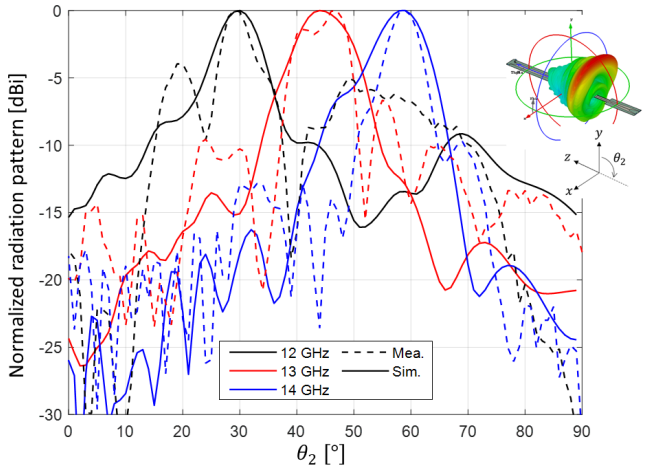

(b) Port 2 excitation.

Fig. 7: Normalized radiation patterns of the Port 1 and Port 2 excitation. The insets are the radiation patterns at 13 GHz.

patterns. After carefully checking the prototype, some vias are not short circuited well causing a broken half TE_{10} mode. Those defect vias worsen the leakage and destroy the uniform leaky radiation.

IV. Conclusion

In this paper, a novel half-mode LWA array is presented. The proposed LWA array has the continuous frequency-scanning in two longitudinal planes, xz and yz planes, and can switch the radiation patterns, bidirectional and unidirectional. The antenna does not need complicated BFN or expensive phase shifters. A prototype was manufactured to verify the performance at the X-band. The feeding network has in-phase and out-of-phase excitations which generate bidirectional (endfire) and unidirectional (broadside) radiation patterns. The two radiation patterns, endfire and broadside, are easily controlled by choosing the feeding ports. SLLs could be further reduced by shaping the aperture of the LWA. In conclusion, the proposed half-mode LWA array provides multiple scanning beams in two orthogonal planes, enriching the traditional LWA's scanning range.

REFERENCES

[1] L. Goldstone and A. Oliner, "Leaky-wave antennas I: Rectangular waveguides," *IEEE Trans. Antennas Propag.*, vol. 7, pp. 307–319, October 1959.

[2] D. R. Jackson and A. A. Oliner, "Leaky-wave antennas," *Modern antenna handbook*, pp. 325–367, 2008.

[3] L. Wang, J. L. Gómez-Tornero, E. Rajo-Iglesias, and O. Quevedo-Teruel, "Low-dispersive leaky-wave antenna integrated in groove gap waveguide technology," *IEEE Trans. Antennas Propag.*, vol. 66, no. 11, pp. 5727–5736, 2018.

[4] A. J. Martinez-Ros, J. L. Gómez-Tornero, V. Losada, F. Mesa, and F. Medina, "Non-uniform sinusoidally modulated half-mode leaky-wave lines for near-field focusing pattern synthesis," *IEEE Trans. Antennas Propag.*, vol. 63, no. 3, pp. 1022–1031, 2014.

[5] S.-L. Chen, D. K. Karmokar, Z. Li, P.-Y. Qin, R. W. Ziolkowski, and Y. J. Guo, "Circular-polarized substrate-integrated-waveguide leaky-wave antenna with wide-angle and consistent-gain continuous beam scanning," *IEEE Trans. Antennas Propag.*, 2019.

[6] D. Sievenpiper, J. Schaffner, J. Lee, and S. Livingston, "A steerable leaky-wave antenna using a tunable impedance ground plane," *IEEE Antennas Wireless Propag. Lett.*, vol. 1, pp. 179–182, 2002.

[7] L. Wang, J. L. Gómez-Tornero, and O. Quevedo-Teruel, "Substrate integrated waveguide leaky-wave antenna with wide bandwidth via prism coupling," *IEEE Trans. Microw. Theory Tech.*, vol. 66, no. 6, pp. 3110–3118, 2018.

[8] J. Xu, W. Hong, H. Tang, Z. Kuai, and K. Wu, "Half-mode substrate integrated waveguide (HMSIW) leaky-wave antenna for millimeter-wave applications," *IEEE Antennas Wireless Propag. Lett.*, vol. 7, pp. 85–88, 2008.

[9] N. Nguyen-Trong and C. Fumeaux, "Half-mode substrate-integrated waveguides and their applications for antenna technology: A review of the possibilities for antenna design," *IEEE Antennas Propag. Mag.*, vol. 60, no. 6, pp. 20–31, 2018.

[10] G. Zelinski, G. Thiele, M. Hastriter, M. Havrilla, and A. Terzuoli, "Half width leaky wave antennas," *IET MICROW ANTENNA P.*, vol. 1, no. 2, pp. 341–348, 2007.

[11] S. Lim, C. Caloz, and T. Itoh, "Metamaterial-based electronically controlled transmission-line structure as a novel leaky-wave antenna with tunable radiation angle and beamwidth," *IEEE Trans. Microw. Theory Tech.*, vol. 53, no. 1, pp. 161–173, 2005.

[12] D. K. Karmokar, Y. J. Guo, P.-Y. Qin, K. P. Esselle, and T. S. Bird, "Forward and backward beam-scanning tri-band leaky-wave antenna," *IEEE Antennas Wireless Propag. Lett.*, vol. 16, pp. 1891–1894, 2017.

[13] J. Liu, D. R. Jackson, and Y. Long, "Substrate integrated waveguide (SIW) leaky-wave antenna with transverse slots," *IEEE Trans. Antennas Propag.*, vol. 60, no. 1, pp. 20–29, 2011.

[14] A. J. Martinez-Ros, J. L. Gómez-Tornero, and G. Goussetis, "Holographic pattern synthesis with modulated substrate integrated waveguide line-source leaky-wave antennas," *IEEE Trans. Antennas Propag.*, vol. 61, no. 7, pp. 3466–3474, 2013.

[15] B. Liu, W. Hong, Y. Q. Wang, Q. H. Lai, and K. Wu, "Half mode substrate integrated waveguide (HMSIW) 3-dB coupler," *IEEE Microw. Wireless Compon. Lett.*, vol. 17, pp. 22–24, Jan 2007.

[16] Q. Lai, C. Fumeaux, W. Hong, and R. Vahldieck, "Characterization of the propagation properties of the half-mode substrate integrated waveguide," *IEEE Trans. Microw. Theory Tech.*, vol. 57, no. 8, pp. 1996–2004, 2009.

[17] Y. J. Cheng, W. Hong, and K. Wu, "Millimeter-wave half mode substrate integrated waveguide frequency scanning antenna with quadri-polarization," *IEEE Trans. Antennas Propag.*, vol. 58, pp. 1848–1855, June 2010.

[18] D. Zheng, Y.-L. Lyu, and K. Wu, "Longitudinally slotted SIW leaky-wave antenna for low cross-polarization millimeter-wave applications," *IEEE Trans. Antennas Propag.*, 2019.

[19] Y. Geng, J. Wang, Y. Li, Z. Li, M. Chen, and Z. Zhang, "Radiation pattern-reconfigurable leaky-wave antenna for fixed-frequency beam steering based on substrate-integrated waveguide," *IEEE Antennas Wireless Propag. Lett.*, vol. 18, no. 2, pp. 387–391, 2019.

[20] Y. Dong and T. Itoh, "Composite right/left-handed substrate integrated waveguide and half mode substrate integrated waveguide leaky-wave structures," *IEEE Trans. Antennas Propag.*, vol. 59, no. 3, pp. 767–775, 2010.

[21] A. J. Martinez-Ros, J. L. Gomez-Tornero, and G. Goussetis, "Planar leaky-wave antenna with flexible control of the complex propagation constant," *IEEE Trans. Antennas Propag.*, vol. 60, no. 3, pp. 1625–1630, 2012.

[22] J. L. Gómez-Tornero, A. J. Martínez-Ros, S. Mercader-Pellicer, and G. Goussetis, "Simple broadband quasi-optical spatial multiplexer in substrate integrated technology," *IEEE Trans. Microw. Theory Tech.*, vol. 63, no. 5, pp. 1609–1620, 2015.

[23] V. G.-G. Buendía, S. K. Podilchak, D. Comite, P. Baccarelli, P. Burghignoli, J. L. G. Tornero, and G. Goussetis, "Compact leaky siw feeder offering tem parallel plate waveguide launching," *IEEE Access*, vol. 7, pp. 13373–13382, 2019.

[24] G.-F. Cheng and C.-K. C. Tzuang, "A differentially excited coupled half-width microstrip leaky EH_1 mode antenna," *IEEE Trans. Antennas Propag.*, vol. 61, no. 12, pp. 5885–5892, 2013.

[25] J. L. Gómez-Tornero, D. Cañete-Rebenaque, and A. Álvarez-Melcón, "Microstrip leaky-wave antenna with control of leakage rate and only one main beam in the azimuthal plane," *IEEE Trans. Antennas Propag.*, vol. 56, no. 2, pp. 335–344, 2008.

[26] A. J. Martinez-Ros, M. Bozzi, and M. Pasian, "Double-sided SIW leaky-wave antenna with increased directivity in the E-plane," *IEEE Trans. Antennas Propag.*, vol. 66, no. 6, pp. 3130–3135, 2018.

[27] D. Zelenchuk, A. J. Martinez-Ros, T. Zvolensky, J. L. Gomez-Tornero, G. Goussetis, N. Buchanan, D. Linton, and V. Fusco, "W-band planar wide-angle scanning antenna architecture," *J. Infrared Millim. Terahertz Waves.*, vol. 34, no. 2, pp. 127–139, 2013.

[28] A. Sarkar, S. Mukherjee, A. Sharma, A. Biswas, and M. J. Akhtar, "SIW-based quad-beam leaky-wave antenna with polarization diversity for four-quadrant scanning applications," *IEEE Trans. Antennas Propag.*, vol. 66, no. 8, pp. 3918–3925, 2018.

[29] M. Poveda-García, D. Cañete-Rebenaque, and J. L. Gómez-Tornero, "Frequency-scanned monopulse pattern synthesis using leaky-wave antennas for enhanced power-based direction-of-arrival estimation," *IEEE Trans. Antennas Propag.*, vol. 67, no. 11, pp. 7071–7086, 2019.

[30] Y. J. Cheng, W. Hong, K. Wu, and Y. Fan, "Millimeter-wave substrate integrated waveguide long slot leaky-wave antennas and two-dimensional multibeam applications," *IEEE Trans. Antennas Propag.*, vol. 59, no. 1, pp. 40–47, 2011.

[31] A. A. Oliner, "A new class of scannable millimeter-wave antennas," in *1990 20th European Microwave Conference*, vol. 1, pp. 95–104, IEEE, 1990.

[32] Y. Li, Q. Xue, E. K. Yung, and Y. Long, "Quasi microstrip leaky-wave antenna with a two-dimensional beam-scanning capability," *IEEE Trans. Antennas Propag.*, vol. 57, pp. 347–354, Feb 2009.

[33] P. Baccarelli, P. Burghignoli, C. Di Nallo, F. Frezza, A. Galli, P. Lampariello, and G. Ruggieri, "Full-wave analysis of printed leaky-wave phased arrays," *INT J RF MICROW C E.*, vol. 12, no. 3, pp. 272–287, 2002.

[34] X. Cao, P. Yang, M. Alzenad, X. Xi, D. Wu, and H. Yanikomeroglu, "Airborne communication networks: A survey," *IEEE J. Sel. Areas Commun.*, vol. 36, no. 9, pp. 1907–1926, 2018.

[35] C. A. Balanis, *Antenna theory: analysis and design*. John wiley & sons, 2016.

[36] Q. Liao, E. Rajo-Iglesias, and O. Quevedo-Teruel, "Ka-band fully metallic TE_{40} slot array antenna with glide-symmetric gap waveguide technology," *IEEE Trans. Antennas Propag.*, vol. 67, no. 10, pp. 6410–6418, 2019.